THE ASTRONOMICAL JOURNAL, 122:2458–2468, 2001

M31 GLOBULAR CLUSTERS IN THE *HUBBLE SPACE TELESCOPE* ARCHIVE. I. CLUSTER DETECTION AND COMPLETENESS[1]

PAULINE BARMBY[2] AND JOHN P. HUCHRA
Harvard-Smithsonian Center for Astrophysics, 60 Garden Street, Cambridge, MA 02138;
pbarmby@cfa.harvard.edu, huchra@cfa.harvard.edu
Received 2001 July 8; accepted 2001 July 19

ABSTRACT

Globular clusters at the distance of M31 have apparent angular sizes of a few arcseconds. While many M31 globular clusters have been detected and studied from ground-based images, the high spatial resolution of the *Hubble Space Telescope* (*HST*) allows much more robust detection and characterization of star cluster properties. We present the results of a search of 157 *HST* Wide Field Planetary Camera 2 images of M31. We found 82 previously cataloged globular cluster candidates, as well as 32 new globular cluster candidates and 20 open cluster candidates. We present images of the new candidates and photometry for all clusters. We assess existing cluster catalogs' completeness and use the results to estimate the total number of globular clusters in M31 as 460 ± 70. The specific frequency is $S_N = 1.2 \pm 0.2$ and the mass specific frequency $T = 2.4 \pm 0.4$; these values are at the upper end of the range seen for spiral galaxies.

Key words: galaxies: individual (M31) — galaxies: star clusters
On-line material: machine-readable tables

1. INTRODUCTION

Globular clusters are among the oldest surviving stellar objects in the universe. They provide collections of Population II stars with homogeneous abundances and histories, and unique stellar dynamical conditions. The Milky Way's globular cluster system (GCS) is the prototypical one, and its study has contributed much to our knowledge of stellar evolution and galactic structure. It is important to make sure that conclusions drawn from this study are not biased either because the Milky Way's GCS is somehow unusual or because our location in the Galaxy prevents us from fully characterizing its properties. Globular clusters in Local Group galaxies are particularly valuable for comparison with Milky Way globular clusters. M31 has the Local Group's largest globular cluster population, so it is a natural starting place for studies of extragalactic globular clusters.

The first M31 globular cluster catalog was published by Hubble (1932), followed by Seyfert & Nassau (1945), Vetešník (1962), Sargent et al. (1977), and Crampton et al. (1985). The most comprehensive recent catalog is that of Battistini et al. (1987); recent works by Battistini et al. (1993) and Mochejska et al. (1998) cover only portions of M31. All these catalogs contain objects that are not M31 globular clusters: for example, Table 2 of Barmby et al. (2000) lists 199 cluster candidates later shown to be nonclusters. The existing catalogs are also likely to be missing clusters as a result of magnitude, spatial coverage, and/or resolution limits. Battistini et al. (1993) defined several samples of M31 globular clusters, including a "confirmed" sample (199 objects), an "adopted best" sample (298 objects), and an "extended" sample (356 objects). In Barmby et al. (2000), we compiled a list of clusters and plausible candidates containing 435 objects.

Quantifying the extent of incompleteness and contamination in M31 globular cluster catalogs is extremely important for the interpretation of GCS properties. For example, the spatial distribution of known clusters is flatter, and their globular cluster luminosity function (GCLF) brighter, near the nucleus (Battistini et al. 1993; Barmby, Huchra, & Brodie 2001b)—is this because the clusters there are truly fewer and brighter, or because existing surveys have not detected the entire cluster population? Even the census of Milky Way clusters is likely to be incomplete: Minniti (1995) estimates that 10–30 Milky Way globular clusters may be hidden behind the Galactic bulge and therefore missing from current catalogs, which list about 150 objects (Harris 1996). Two such clusters were found by Hurt et al. (2000). It is not unreasonable to suspect that the M31 cluster catalogs could be incomplete by at least a similar fraction.

Ground-based high-resolution imaging and spectroscopy have been used to distinguish M31 globular clusters from interlopers such as foreground stars, background galaxies, and other objects belonging to M31 (e.g., H II regions and open clusters). The bright ($V \lesssim 17$) portion of M31 globular cluster catalogs has been fairly thoroughly examined using one or both of these methods. Racine (1991) and Racine & Harris (1992) used short-exposure CCD images taken in excellent seeing to determine whether cluster candidates in the M31 halo were resolved into stars; they found that majority of the halo cluster candidates were background galaxies, not clusters. Radial velocities from optical spectroscopy have also been used by several groups (e.g., Huchra, Stauffer, & Van Speybroeck 1982; Federici, Marano, & Fusi Pecci 1990; Huchra, Brodie, & Kent 1991; Federici et al. 1993; Barmby et al. 2000) to eliminate background galaxies and foreground stars from cluster candidate lists. Neither method is infallible, however: compact clusters may be mistaken for background galaxies if not

[1] Based on observations made with the NASA/ESA *Hubble Space Telescope*, obtained from the data archive at the Space Telescope Science Institute. STScI is operated by the Association of Universities for Research in Astronomy, Inc., under NASA contract NAS 5-26555.

[2] Guest User, Canadian Astronomy Data Centre, which is operated by the Herzberg Institute of Astrophysics, National Research Council of Canada.

resolved into stars, or for stars if they have a small radial velocity.[3] *Hubble Space Telescope* (*HST*) imaging, with its superior spatial resolution, is a useful tool for removing some of the ambiguities inherent in the ground-based studies.

At the distance modulus of M31 given by Stanek & Garnavich (1998) and Holland (1998) [$(m - M)_0 = 24.47$, $d = 783$ kpc], the angular resolution of *HST*'s Wide Field Planetary Camera 2 (WFPC2) is equivalent to a spatial resolution of 0.38 pc, very helpful for the identification of globular clusters in M31. The differences between globular clusters and contaminating objects are much more obvious than with ground-based imaging. M31 has been a popular target for *HST*: as of 2000 December 1, the Hubble Data Archive contained almost 1100 WFPC2 images within 150′ of the center of the galaxy. As of the same date, about two dozen M31 globular clusters had been specifically targeted for observation with *HST*, and the images of these clusters make up about 20% of all the M31 images. The goal of most targeted *HST* observations of M31 globular clusters has been the production of color-magnitude diagrams for the clusters and surrounding stellar populations. *HST* programs that specifically targeted M31 globular clusters include GO 5112, 5420, 5464, 5907, 6477, 6671, 7826, 8296, and 8664. Our study uses the publicly available archival data from these programs and many others.

In mid-2000, we began a project to search for globular clusters in archival *HST* images for the purpose of quantifying the incompleteness of existing cluster catalogs; preliminary results were described in Barmby et al. (2001b). The present paper reports the results of our efforts to find globular and other star clusters in archival *HST* WFPC2 images, and their implications for catalog completeness and contamination. A follow-up paper (Barmby, Holland, & Huchra 2001a) presents measurements of the structural parameters of the clusters and their implications. We do not attempt to construct color-magnitude diagrams for the clusters, since this work is already being carried out by other groups.

2. SEARCHING THE *HST* ARCHIVE

We searched the *HST* archive for all WPFC2 observations with the following properties:

1. Center of field within 150′ of the center of M31;
2. Broadband filter with central wavelength of 300 nm or longer;
3. Total exposure time longer than 100 s.

These parameters were chosen to ensure that we would have a reasonable chance of detecting globular clusters if they were in the image fields. Many images met the requirements, but since most positions had more than one observation per filter and observations in more than one filter, the images comprised only 157 separate fields. Some of these fields were known to contain M31 globular clusters; we retained these fields in our search as a check on our ability to identify clusters. We searched the images in only one filter per field. If more than one filter was available, we chose filters in the following order: F555W, F814W, F606W, F450W, F439W, F336W, F300W (this ordering reflects the distribution of filters used for the images, combined with our desire to examine as many fields as possible in the same filter). Information on the fields searched, including data set name, location, filter, and exposure time, is given in Table 1. The images searched are mostly in F555W and F814W, although there is at least one image in each of the filters listed above. The exposure times ranged from 100 to 8400 s. Figure 1 shows the location of all fields on the sky.

We retrieved the images from either the Space Telescope Science Institute (STScI) or the Canadian Astronomy Data Centre (CADC). In both cases, the images were pipeline-processed from the raw data at the time of retrieval with the best available calibration images. From STScI we retrieved individual *HST* images; when multiple images existed for a single field (e.g., in the case of "cosmic-ray split" images), we combined the images using the IRAF task CRREJ. From CADC we retrieved "WFPC2 associations"; these

TABLE 1

HST FIELDS USED IN THE SEARCH

R.A. (J2000)	Decl. (J2000)	Filter	Exposure (s)	Data Set Name
00 32 36.21	+39 27 43.4	F606W	1400	U4K2OI01R
00 32 36.62	+39 27 42.0	F606W	1500	U4K2OI02R
00 32 49.01	+39 35 00.4	F555W	1600	U2E20709T
00 34 13.68	+39 23 26.5	F814W	2800	U2TA0501T
00 34 13.26	+39 23 48.4	F555W	600	U4490401R

NOTE.—Table 1 is presented in its entirety in the electronic edition of the Astronomical Journal. A portion is shown here for guidance regarding its form and content. Units of right ascension are hours, minutes, and seconds, and units of declination are degrees, arcminutes, and arcseconds.

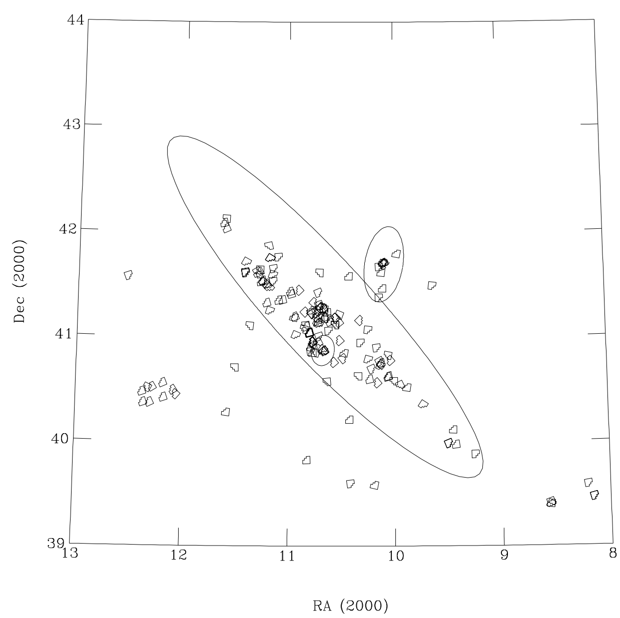

FIG. 1.—Location and orientation of M31 *HST* fields. The large ellipse is the M31 disk-halo boundary as defined by Racine (1991); smaller ellipses are D_{25} isophotes of NGC 205 (northwest) and M32 (southeast). The WFPC2 symbols are drawn about 1.5 times actual size to make them easier to see. The group of fields at R.A. ∼ 12°, decl. ∼ 40°.5 is part of a snapshot survey of field galaxies (GO 6354).

[3] Recall that M31 has a heliocentric radial velocity $v_r \approx -300$ km s^{-1}. The velocity range of M31 globular clusters is about +70 to −700 km s^{-1}, and the Galactic models of Ratnatunga, Bahcall, & Casertano (1989) predict that the radial velocities of Milky Way stars with similar colors and magnitudes to M31 globular clusters are in the range −400 to +100 km s^{-1}.

are co-added images produced by the CADC pipeline, which combines multiple CR-SPLIT images with the GCOMBINE task. We found that GCOMBINE did not adequately remove cosmic-ray hits when only two images were co-added, so in that case we retrieved the individual images and combined them with CRREJ. There were no obvious differences in the images produced using the two methods—we used both since we became aware of the availability of association images from the CADC partway into the project.

Once the images were processed, we began the search for star clusters. The first step was carried out "blind," that is, without any knowledge of the positions of cataloged clusters. Working independently, each of us visually examined each image. P. B. used SExtractor (Bertin & Arnouts 1996) to automatically identify objects with large areas and/or extended profiles and then visually checked the SExtractor candidates (many of these were actually bright stars) and searched for additional candidates. J. P. H. used only visual examination of the images. Bright M31 globular clusters can be visually distinguished from stars and elliptical galaxies because they appear more "ragged" at the edges (being resolved into stars) and do not have the diffraction spikes seen around bright stars. Faint or small clusters are distinguished more by their image shapes—larger than the point-spread function, and less smooth than a galaxy—than by resolution into stars. Clusters are distinguished from H II regions or nebulae by the fact that the latter are much more diffuse and show few individual stars. The visual classification is not completely objective, but it was the best method we could contrive for dealing with the large number of images to be examined and the large number of potential contaminating objects.

Our confidence in the visual classification was bolstered by the fact that we only disagreed on the classification of about 10% of the objects. We reexamined these together to make a final classification. We combined our two lists of cluster candidates to make a final list. Although we were interested primarily in globular clusters, we recorded positions of possible open clusters as well. Following previous authors (e.g., Battistini et al. 1987; Mochejska et al. 1998), we classified our globular clusters into classes A through D, where A is "very likely to be a globular cluster" and D is "likely not a globular cluster." We refer to objects in classes A and B as good candidates, and objects in classes C and D as marginal cluster candidates. After generating our final list of cluster candidates, we checked the image positions against existing catalogs of M31 globular clusters. This allowed us to gauge our detection efficiency and locate objects we would otherwise have missed. The globular cluster list used was a "master list" of globular clusters and candidates, produced by combining the lists of Sargent et al. (1977), Crampton et al. (1985), Battistini et al. (1987, 1993), and Mochejska et al. (1998); it includes all the objects listed in the Barmby et al. (2000) catalog, plus additional low-probability candidates and nonclusters.

3. SEARCH RESULTS

3.1. *Globular Clusters*

We consider the low- and high-probability globular clusters separately. "High probability" are A- or B-class clusters from Battistini et al. (1987, 1993) or Mochejska et al. (1998); all other objects are "low probability." Racine (1991) showed that the Battistini et al. (1987) classification correlates well with the probability that a candidate will subsequently be shown to be a cluster. Seventy-five high-probability clusters from our master list were located in the *HST* fields; we detected 71, and some images of previously cataloged clusters are shown in Figure 2. Three of the four nondetections (138-000, 166-000, and 133-191) appeared to be stars or blends of stars rather than globular clusters; the fourth object was DAO 40, and we did not detect any object at the coordinates given by Crampton et al. (1985). Of the 72 low-probability (class C or D) cluster candidates in our *HST* fields, we found seven good candidates (000-D038, 000-M91, 020D-089, 097D-000, 132-000, 264–NB 19, and NB 39), four marginal candidates (000-M045, 257-000, NB 41, and NB 86), and 45 objects that did not appear to be clusters. We did not detect the other 14 objects in our visual search. On reexamining the positions of these objects, we found that none were good or even marginal cluster candidates. Several were clearly stars, and the others were blends of stars or blank fields. Table 2 gives a list of the nonclusters and their classifications.

3.2. *Uncataloged Globular Clusters*

Our visual search of the *HST* fields produced 32 objects not included in any cluster catalog. Ten of these were good candidates, although only about half are as obviously clusters as most of the brighter objects. The good candidates' images are shown in Figure 3. The nature of the remaining 22 objects is unclear. They are clearly not stars; all are at least marginally resolved (FWHM $\gtrsim 0''.2$). However, most are quite faint, and they are not obviously resolved into stars as is the case for most of the globular clusters. They may be blended stars in M31, compact background galaxies, or compact star clusters. We show images of these low-quality objects in Figure 4. Table 3 gives the location and quality of all the new cluster candidates.

3.3. *Open Clusters*

The dividing line between open and globular clusters is somewhat blurred, even in the Milky Way. In their compilation of data on Milky Way globular clusters, Djorgovski & Meylan (1993) note that there are several globular clusters (BH 176, UKS 2) that could instead be open clusters. In our search, we noted several concentrated objects that could be M31 open clusters. Their nature is uncertain: they could also be low-concentration globular clusters, or just chance superpositions of stars. Their images are shown in Figure 5. We checked the cluster coordinates against those given in Hodge's (1979) list of M31 open clusters. The

TABLE 2

CATALOGED OBJECTS THAT ARE NOT M31 GLOBULAR CLUSTERS

Name	Class	*HST* Field(s)
000-253	Star	U2M80H01T[4]
000-M046......	H II region?	U2Y20106T[2]
000-M050......	H II region?	U4WOBH08A[4]
000-M068......	Stars	U4F51407A[4]
000-V211	Stars	U2TR0804B[4]

NOTE.—Table 2 is presented in its entirety in the electronic edition of the Astronomical Journal. A portion is shown here for guidance regarding its form and content.

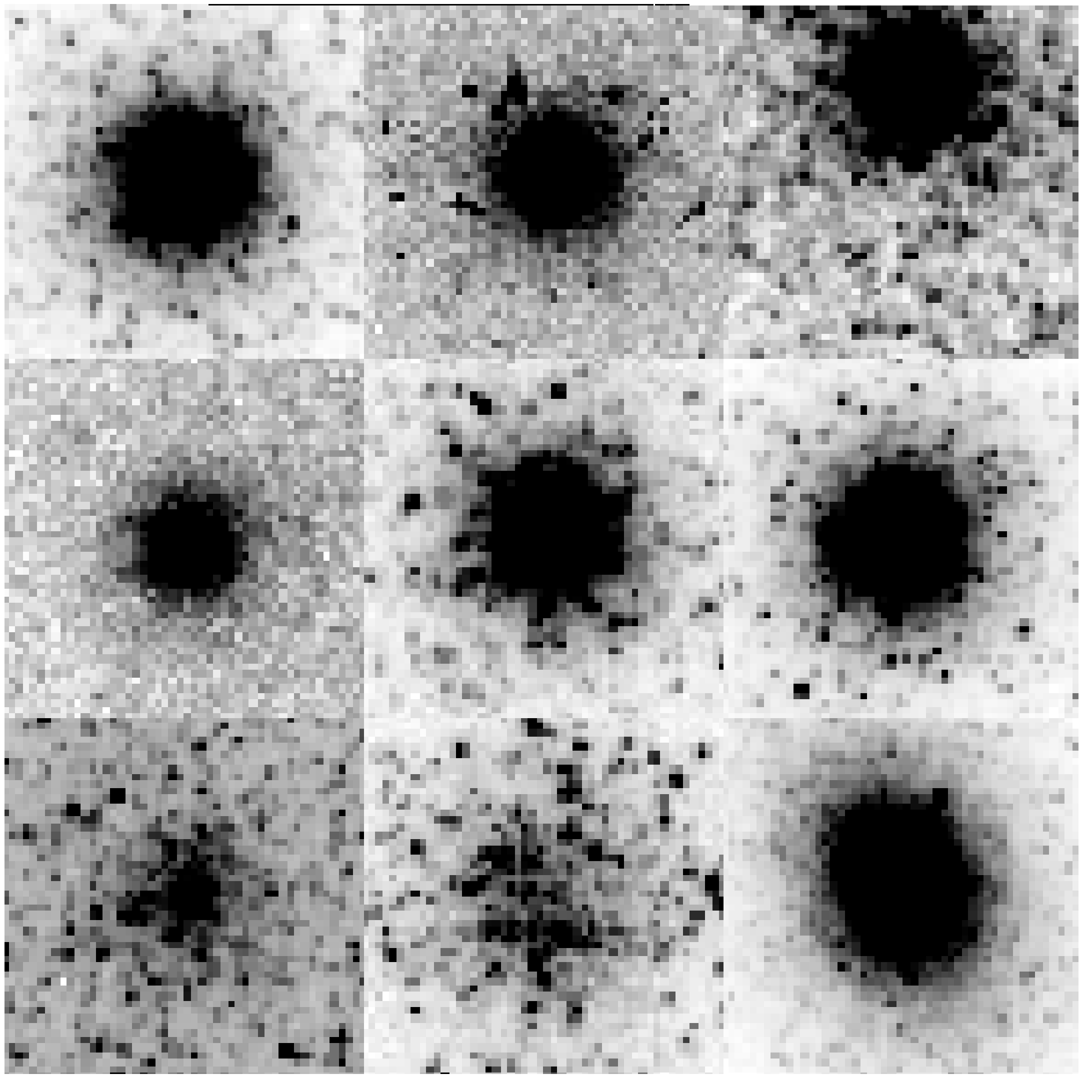

FIG. 2.—*HST* images of M31 globular clusters. In row order, from top left: 006-058, 064-125, 077-138, 146-000, 156-211, 311-033, 331-057, 468-000, and 000-001. All images are in filter F555W or F606W except those of 064-125 and 146-000 (in F300W). All images are 5″ square; 077-138 is not centered in its image because it fell near the edge of a WFPC2 chip.

coordinates in that catalog have rather low precision (20″ in both right ascension and declination), so we searched for coordinate matches within an error circle of radius 30″. We found five matches and attempted to confirm these by comparing the finding charts in Hodge (1982) with our images. The results were inconclusive; either the objects were not clearly identified on the charts or they were located too close to the edge of the *HST* image to make a positive identification. We note the possible matches in Table 3.

To see if any of our newly proposed globular and open cluster candidates had been previously cataloged as background galaxies, we checked their positions against those of galaxies listed in NED.[4] None of the new clusters matched the position of any galaxy listed in NED, although one is listed as a possible H II region (Strauss et al. 1992) and two others may contain radio and X-ray sources (Zhang et al. 1993; Supper et al. 1997). The matches are also noted in Table 3. However, the matches are uncertain, since positional uncertainties for the other surveys are large. Figure 6 shows the positions on the sky of all the M31 clusters, both previously known and newly discovered. The "open cluster" near NGC 205 is well outside the disk and is probably not a real cluster.

4. INTEGRATED PHOTOMETRY

After the M31 clusters had been identified on the "search" images, we retrieved images of their fields in other available filters to extract the most photometric information from the *HST* archive. All but 18 clusters had been imaged by WFPC2 in more than one filter. We combined images for cosmic-ray rejection in the same manner used for the search images. Additional processing steps included removing cosmic rays interactively using the IRAF task IMEDIT (this was especially important for images that were not cosmic-ray split) and correcting for warm pixels using the IRAF task COSMICRAYS. While the STSDAS task WARMPIX is the preferred method of dealing with warm pixels, it is slow and requires correction of individual images before they are combined for cosmic-ray rejection.

[4] The NASA/IPAC Extragalactic Database (NED) is operated by the Jet Propulsion Laboratory, California Institute of Technology, under contract with the National Aeronautics and Space Administration.

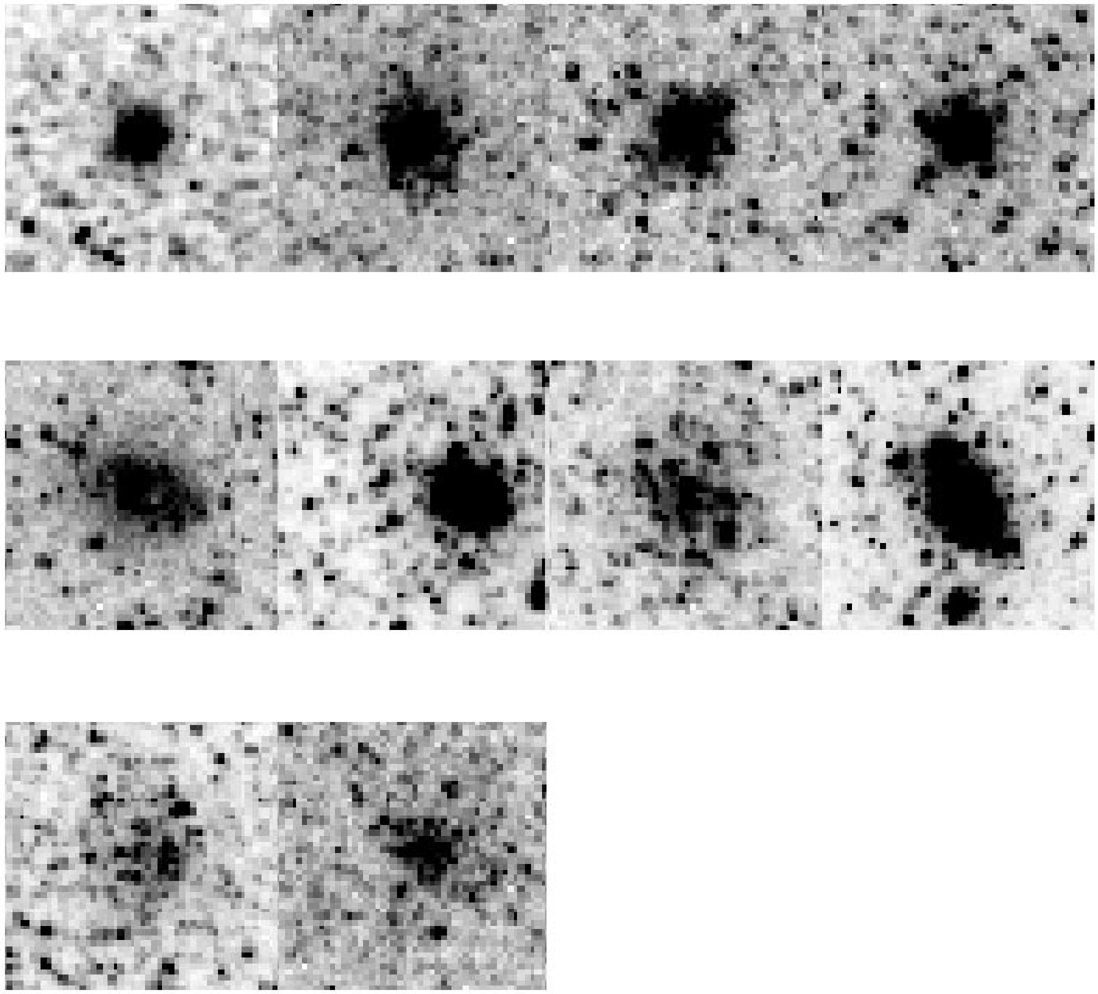

FIG. 3.—New globular cluster candidates found in *HST* images. All images are 5″ square.

Since we had hundreds of individual images to deal with, we chose the more expedient method of treating the warm pixels as if they were cosmic-ray hits on ground-based images. Nearby bright stars and CCD flaws were masked out of the images to prevent contamination of the photometry. A few images were not useful for photometry at all: the globular clusters were either very faint (mostly in the F300W and F336W filters), too close to an image edge, or saturated.

Photometry of extragalactic globular clusters is unfortunately not as simple as photometry of isolated stars or galaxies. There are two key steps in integrated photometry of M31 clusters: measuring the background light, and identifying an appropriate aperture size. The background light consists of two components: unresolved light from the sky and M31, and light from resolved stars in M31 (the latter are a lesser problem in ground-based photometry of M31 globular clusters, since many fewer M31 stars are resolved). Standard background estimators are usually designed to determine the sky background level by rejecting the stars in the background annulus. Since we expect there to be stars overlapping our clusters as well, we estimated the background value for each image as the mean (rather than the more commonly used median or mode) of the pixel values around the image edge and subtracted it from the image before doing photometry.

Determining the "correct" aperture size to be used for integrated photometry is nontrivial, since the clusters are not all the same size. We estimated the total flux for each object by measuring aperture magnitudes in concentric apertures spaced 0.″15 apart, plotting magnitude growth curves, and noting where the flux stopped increasing. Using these measurements of the total flux of each cluster, we determined the half-light radius[5] by interpolating the aperture magnitude curves. We calibrated the instrumental magnitudes from the WFPC2 system to the standard system by iteratively solving the equations given in Holtzman et al. (1995), using the charge transfer efficiency corrections given by Dolphin (2000). The iterative solution of the calibration equations requires instrumental magnitudes in at least two filters; for objects with only one instrumental magnitude, we fixed the "standard color" as either the measured ground-based color from Barmby et al. (2000) or, if that was unavailable, the average M31 globular cluster color. The results for integrated magnitudes and half-light radii are given in Table 4. In Figure 7, we compare the new

[5] The half-light radius r_h is that which contains half of the integrated cluster light. It should not be confused with the radius at which the surface brightness drops to half of its central value, called variously the core radius r_c, the half-intensity radius, or the half-width at half-maximum (HWHM).

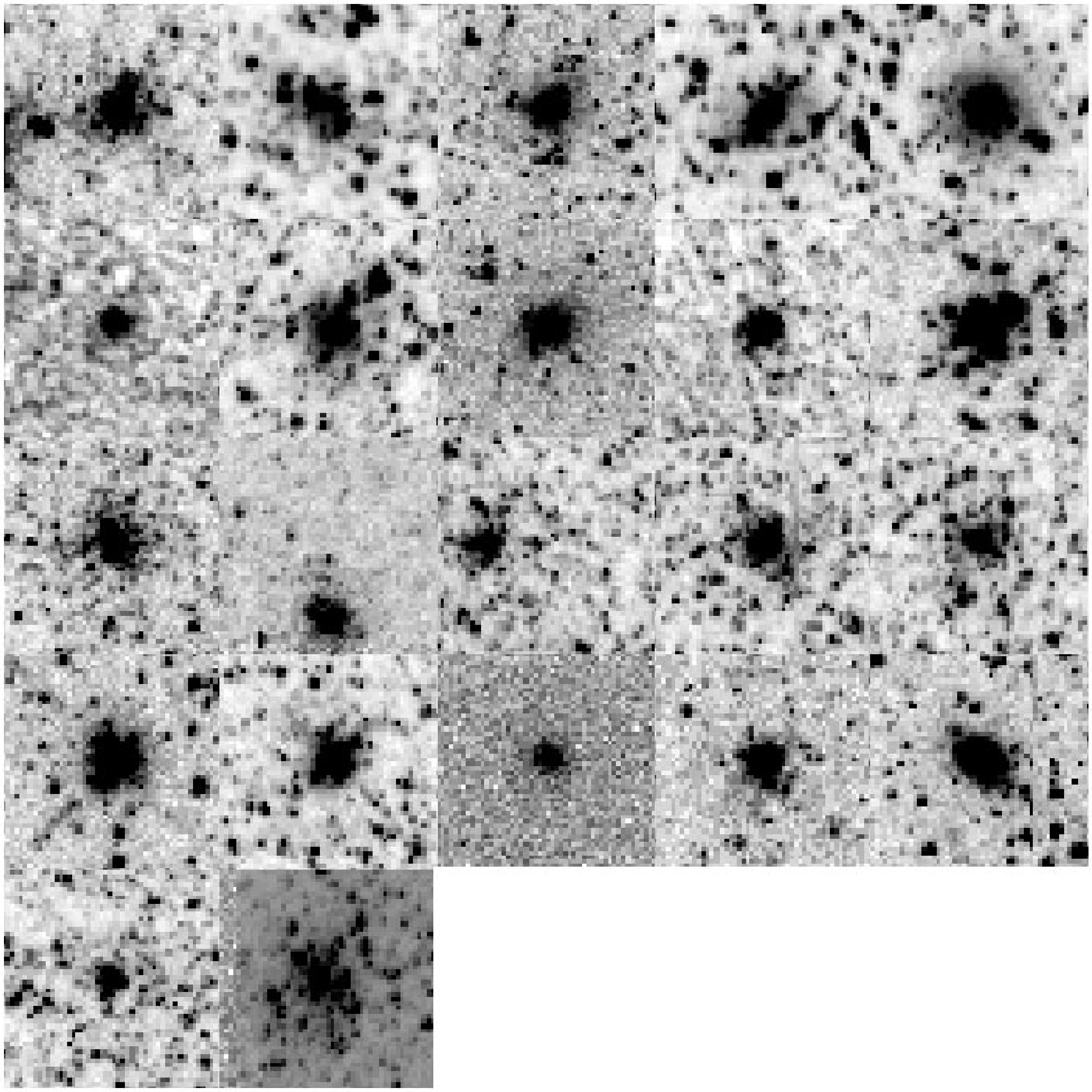

FIG. 4.—Marginal objects found in *HST* images: these objects are nonstellar but not obviously star clusters. All images are 5″ square.

HST photometry with the ground-based measurements compiled in Barmby et al. (2000). The agreement is gratifying: the median offset in V is 0.01 ± 0.04 mag, and that in I is 0.06 ± 0.04 mag. Most of the large offsets are for objects near the edge of a WFPC2 chip, or whose previous photometry was estimated from photographic plates.

5. COMPLETENESS OF GLOBULAR CLUSTER CATALOGS IN M31

To estimate the completeness of globular cluster catalogs in M31, we first need to understand our own detection efficiency. We estimated this by inserting artificial globular clusters into the inner images, for which the distance from the center of M31, R_{gc}, was less than 30′. The artificial clusters were actually images of the brightest real globular clusters we detected. To insert the artificial clusters, we scaled the image fluxes 0–4 mag fainter, adjusted for the exposure time of the inserted image, rotated the cluster to a random position angle, and applied a random axial ratio from 0.85 to 1.0. This may not have been an entirely correct method of generating artificial clusters, since cluster size, surface brightness, and integrated magnitude are known to be correlated for Milky Way clusters. However, we decided that it was better not to introduce additional assumptions about the correlation of these parameters into our detection test. Once an artificial cluster was inserted into a copy of each *HST* frame, we extracted a 15″ × 15″ region around the inserted cluster and examined only that portion of the image. This cutout procedure was similar to the procedure used for the reexamination of "problem" images. In fact, the visual examination of the two groups of images was done at the same time, with no reference to which were the inserted clusters and which were the real objects. For each cutout image, we decided whether or not it was a bona fide globular cluster.

The results of our search for the inserted globular clusters are in Figure 8, where detection of each inserted cluster is indicated as a function of V magnitude and R_{gc}. The figure shows, as expected, that our detection efficiency was generally worse for fainter objects and objects near the center of M31. Faint clusters are more difficult to find against the bright background of the M31 disk and nucleus. We also failed to detect a few bright objects, mostly in short exposures or in the near-UV filters F300W and F336W. Overall,

TABLE 3

NEW GLOBULAR CLUSTER CANDIDATES FOUND IN M31 *HST* FIELDS

Name	R.A. (J2000)	Decl. (J2000)	Quality	Comment
M31GC J003411+392359......	00 34 11.48	39 23 59.1	C/D	
M31GC J004010+403625......	00 40 10.33	40 36 24.7	C/D	
M31GC J004023+414045......	00 40 22.68	41 40 44.5	C	
M31GC J004027+414225......	00 40 27.25	41 42 24.8	B	
M31GC J004030+404530......	00 40 30.46	40 45 29.6	B	
M31GC J004031+404454......	00 40 30.63	40 44 54.3	C	
M31GC J004031+412627......	00 40 30.68	41 26 27.1	C	
M31GC J004034+413905......	00 40 34.42	41 39 04.8	C/D	
M31GC J004037+403321......	00 40 37.15	40 33 21.4	C	
M31GC J004045+405308......	00 40 44.92	40 53 07.6	C	
M31GC J004051+404039......	00 40 50.68	40 40 38.6	B/C	
M31GC J004103+403458......	00 41 02.88	40 34 57.9	B	Hodge 119?
M31GC J004146+413326......	00 41 45.57	41 33 26.2	C	
M31GC J004200+404746......	00 42 00.39	40 47 45.8	C	
M31GC J004228+403330......	00 42 27.56	40 33 29.8	C/D	
M31GC J004246+411737......	00 42 46.01	41 17 36.5	C	
M31GC J004251+405841......	00 42 50.80	40 58 40.7	C	
M31GC J004251+411035......	00 42 50.78	41 10 34.7	A	
M31GC J004257+404916......	00 42 57.05	40 49 16.4	C	Hodge 195?
M31GC J004258+405645......	00 42 58.02	40 56 45.4	A	
M31GC J004301+405418......	00 43 01.35	40 54 17.5	B	
M31GC J004304+405129......	00 43 04.27	40 51 29.2	C	
M31GC J004304+412028......	00 43 03.75	41 20 28.2	A	
M31GC J004312+405303......	00 43 11.86	40 53 02.8	B	
M31GC J004312+410249......	00 43 11.99	41 02 49.1	C	
M31GC J004424+414502......	00 44 23.71	41 45 02.3	C	X-ray source; SHP 278?
M31GC J004425+414529......	00 44 25.21	41 45 29.1	C/D	
M31GC J004439+414426......	00 44 39.07	41 44 26.3	C	
M31GC J004537+413644......	00 45 37.25	41 36 44.3	B	
M31GC J004537+414332......	00 45 36.75	41 43 32.2	C	
M31GC J004622+420631......	00 46 21.80	42 06 30.8	C	
M31GC J004624+420059......	00 46 23.50	42 00 58.5	C	
M31OC J003836+412739......	00 38 35.73	41 27 39.3	B	
M31OC J003941+403154......	00 39 40.52	40 31 53.6	C	
M31OC J003943+403116......	00 39 43.21	40 31 15.6	C	
M31OC J004000+403326......	00 39 59.99	40 33 25.9	C	
M31OC J004008+403507......	00 40 07.55	40 35 06.6	B	
M31OC J004027+404524......	00 40 27.26	40 45 23.7	C	
M31OC J004031+404537......	00 40 30.51	40 45 37.4	C	
M31OC J004053+403519......	00 40 52.94	40 35 19.2	D	
M31OC J004054+404625......	00 40 54.14	40 46 24.7	C	
M31OC J004057+403425......	00 40 56.62	40 34 24.7	C	
M31OC J004119+403608......	00 41 18.69	40 36 08.2	B/C	
M31OC J004123+403756......	00 41 23.30	40 37 56.1	C	
M31OC J004421+414516......	00 44 21.44	41 45 15.9	C	
M31OC J004442+415122......	00 44 41.84	41 51 22.4	C	
M31OC J004442+415237......	00 44 42.25	41 52 36.7	C	
M31OC J004449+414430......	00 44 48.83	41 44 30.3	C/D	
M31OC J004450+415211......	00 44 50.27	41 52 11.1	C	
M31OC J004510+413646......	00 45 10.45	41 36 46.3	C	Hodge 311?
M31OC J004512+413712......	00 45 11.81	41 37 11.6	C	H II region; Hodge 313?
M31OC J004539+414220......	00 45 38.88	41 42 20.4	C	Radio source; MY 0042+414?

we correctly identified 80% of the inserted clusters and 92% of the objects that appeared in long F555W and F814W exposures.

The distribution of the real globular clusters and candidates detected in the *HST* images is shown in Figure 9. The number of newly detected objects increases at fainter magnitudes; there is no clear trend in the number of new objects with R_{gc}. We use the data in Figures 8 and 9 to estimate the completeness of existing catalogs. While it would be desirable to estimate the completeness as a joint function of magnitude and position, the small number of objects we have to work with makes deriving $C(V, R_{gc})$ difficult. Instead we summed over one variable to produce separate functions $C(V)$ and $C(R_{gc})$, which are plotted in Figure 10. The catalog completeness is computed by dividing the number of cataloged objects in a given bin by the true

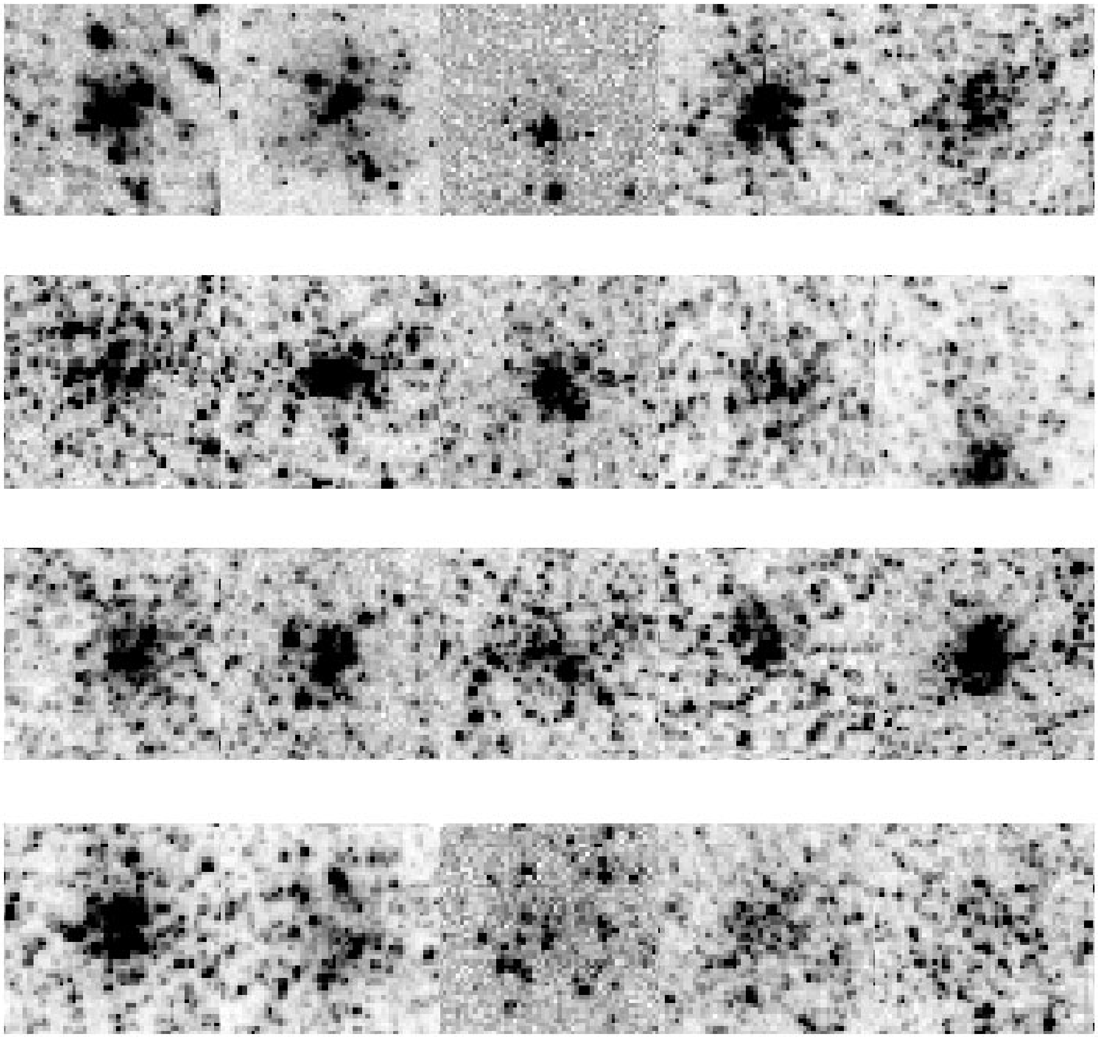

FIG. 5.—Possible M31 open clusters found in *HST* images. All images are 5″ square.

number of objects:

$$C = \frac{N_{\rm cat}}{N_{\rm true}} = \frac{N_{\rm cat}}{N_{\rm cat} + N_{\rm new}/\eta}\ , \quad (1)$$

where the "true" object total is the sum of the number of cataloged objects and the number of new objects divided by our detection efficiency η. The number of new objects includes the marginal objects. From the results of Racine (1991), only a fraction ($f \lesssim 0.5$) of the marginal objects are likely to be true globular clusters. We therefore give a range of solutions for the completeness functions in Figure 10, corresponding to $f = 0$, 0.5, and 1.0. The figure shows, as expected, that existing catalogs are reasonably complete to $V = 18$, after which the completeness drops drastically. To compute the completeness as a function of $R_{\rm gc}$, we assumed that detection efficiency at $R_{\rm gc} > 30'$ was the same as that in the $R_{\rm gc} = 30'$ bin. The completeness as a function of $R_{\rm gc}$ does not follow any particular pattern; the most important point is the low completeness in the innermost bin. $C(R_{\rm gc})$ can only be measured out to about $R_{\rm gc} \leq 70'$, and averaging over this region yields values for the overall completeness of 50%–85%. The small number of objects per radial bin and the uncertainty about the nature of the marginal objects make this estimate rather imprecise.

TABLE 4

PHOTOMETRY OF NEW CLUSTERS AND CANDIDATES IN M31 *HST* FIELDS

Name	U[a]	B	V	R	I	$\langle r_h \rangle$ (arcsec)
Cataloged clusters:						
000-001	...	...	13.807	...	12.684	0.40
000-D38	...	...	19.247	...	18.276	0.37
000-M045......	...	19.391	18.723	...	17.446	1.49
000-M91	...	...	19.143	...	...	0.89
006-058	...	...	15.463	...	14.354	0.38

NOTE.—Table 4 is presented in its entirety in the electronic edition of the Astronomical Journal. A portion is shown here for guidance regarding its form and content.

[a] Asterisks indicate F300W, instead of standard U-band, magnitudes.

It is important to know the total number of globular clusters in M31, since it is one of the few spiral galaxies with a well-studied GCS. Existing surveys (summarized in Barmby et al. 2000b) and our new *HST* survey bring the number of confirmed M31 globular clusters to over 250. The most comprehensive attempt to estimate the total number of M31 globular clusters (Battistini et al. 1993) gives population ratios $N_{\rm M31}/N_{\rm MW} = 2.5$–3.5; with $N_{\rm MW} = 150$, this gives $N_{\rm M31} = 375$–525, or 450 ± 75. We can use the results of our completeness study to attempt a new

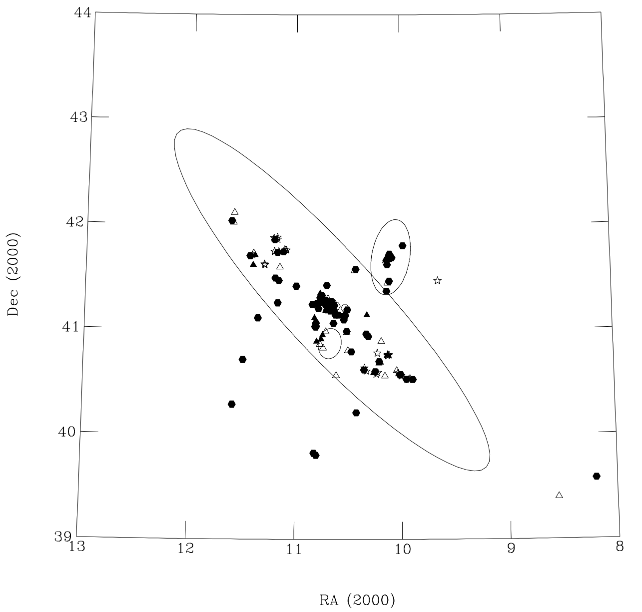

FIG. 6.—Position on the sky of all globuar clusters, globular cluster candidates, and open clusters. Ellipses are the same as in Fig. 1. Filled symbols are good-quality globular cluster candidates; open symbols are marginal candidates. Hexagons are previously cataloged objects; triangles are newly discovered objects; stars are possible open clusters.

estimate of the total number of M31 globular clusters. We take two approaches, which use the completeness data somewhat differently. One approach is to use the result that for $V < 18$ and $R_{gc} > 5'$, the existing sample is close to complete. We can therefore use the results of GCLF fitting in this region to estimate the number of clusters fainter than $V = 18$. The GCLFs computed in Barmby et al. (2001) give a total number of clusters N_{gc} in the range 394–417; the midpoint of the range is 406. In the region $R \leq 5'$, there are 37 cataloged clusters or candidates, and the catalog com-

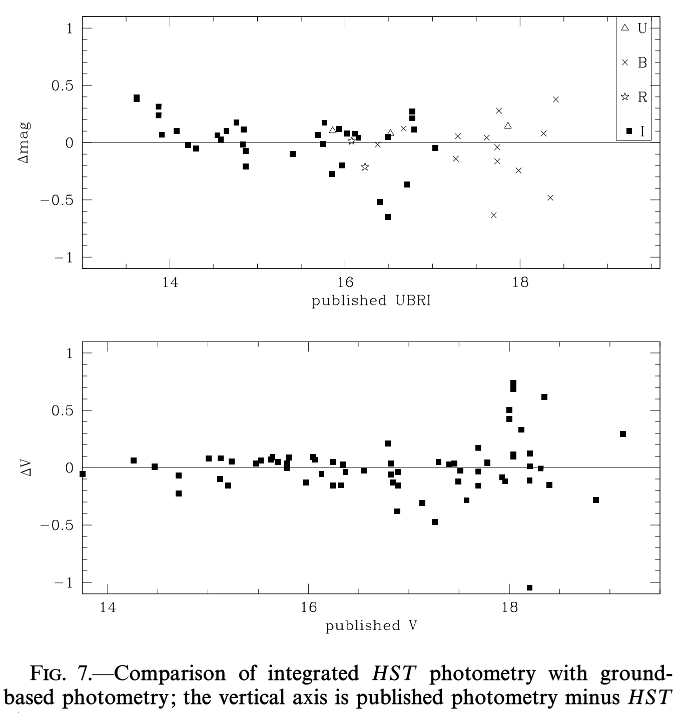

FIG. 7.—Comparison of integrated *HST* photometry with ground-based photometry; the vertical axis is published photometry minus *HST* photometry.

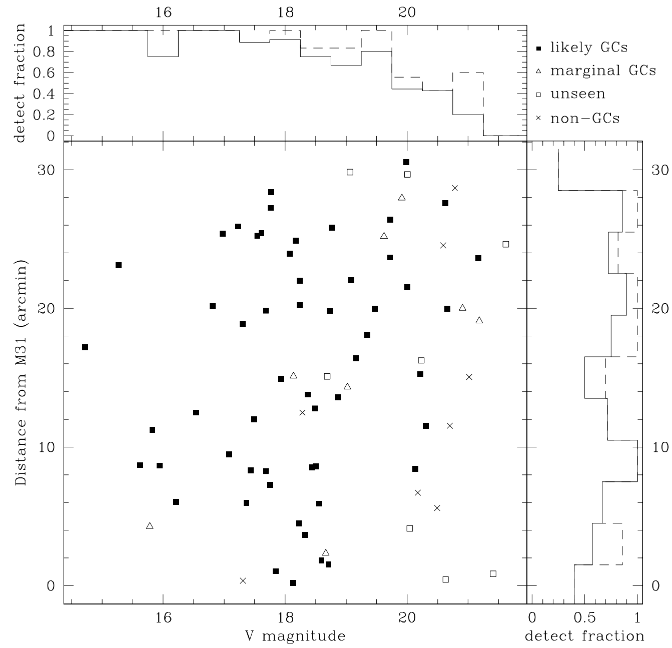

FIG. 8.—Measurement of globular cluster detection efficiency. *Large plot*: V magnitude vs. R_{gc} for artificial clusters. Symbol type indicates whether an object was detected and how it was classified. The histograms are the fraction of inserted objects detected; solid lines include only A- or B-class ("good") globular clusters, and dashed lines include marginal objects.

pleteness is about 70%. This implies that the true number of clusters is about 53, so the total number of globular clusters in M31 is approximately $406 + 53 = 459$. A reasonable estimate of the error in this value is 15%, or ± 69.

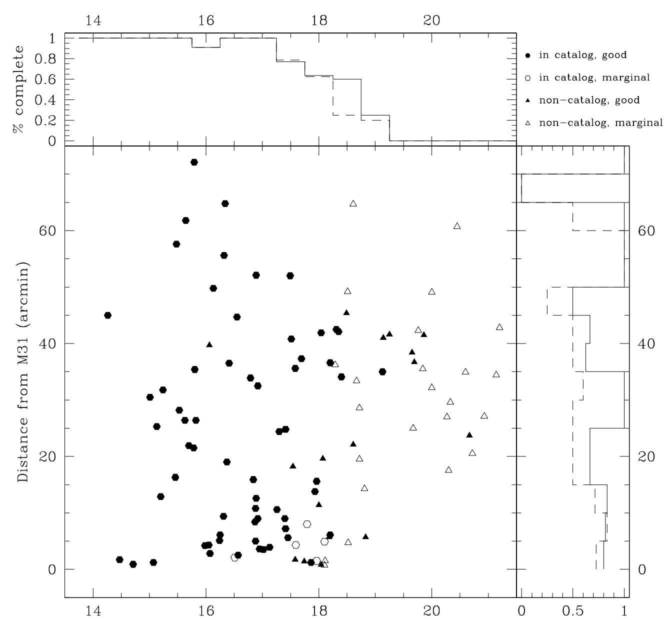

FIG. 9.—Location of previously cataloged and newly discovered M31 globular clusters in V vs. R_{gc} space. Symbols indicate object quality and presence in existing catalogs. Histograms estimate the existing catalogs' completeness by showing the number of previously known objects per bin divided by the sum of the number of known and the number of new objects per bin. Solid histograms include only A- or B-class globular clusters, and dashed histograms include marginal objects.

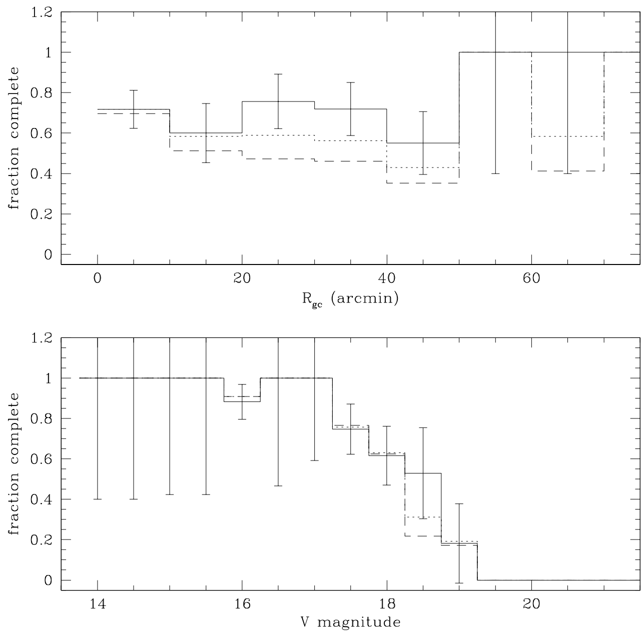

FIG. 10.—Completeness functions for existing surveys of globular clusters in M31. The top panel, $C(R_{gc})$, is summed over entire magnitude range, and the bottom panel, $C(V)$, is summed over the entire radial range. Different line styles reflect different assumptions about how many marginal objects are true M31 clusters: *solid lines*, none; *dotted lines*, half; *dashed lines*, all.

We can also use the completeness estimates directly, to estimate

$$N_{gc} = \sum_{R_{gc}} \frac{N_{good} + f N_{marg}}{C(R_{gc})}, \tag{2}$$

where N_{good} and N_{marg} are the number of good and marginal cataloged clusters in a given R_{gc} bin. The C used in the computation is the value plotted in Figure 10 for the appropriate value of f. The catalog used is that given by Barmby et al. (2000) with likely NGC 205 clusters and (likely young) blue clusters removed. The 299 good clusters are those confirmed by spectroscopy or high-resolution imaging and/or members of the "adopted best sample" of Battistini et al. (1993); the other 130 clusters are considered marginal. The resulting N_{gc} is sensitive to the value of f and ranges from 415 ± 57 for $f = 0$ to 856 ± 126 for $f = 1.0$. A value of $f = 0.25$, which we believe is reasonable, yields $N_{gc} = 494 \pm 45$. Our two estimates of the total number of globular clusters in M31 are compatible both with each other and with the results of Battistini et al. (1993). The precision of our results is not much better than that of previous estimates, and improvement will require a wide-field, deep CCD survey of M31 that can be used to find globular clusters in a uniform manner across the galaxy; such a survey is currently being carried out (Lee et al. 2001).

We now consider implications of our estimated value of M31's N_{gc} for its specific frequency S_N and "mass specific frequency" T (Zepf & Ashman 1993). To do this we need values for M31's luminosity and mass-to-light ratio. Kent (1987) gives the total magnitude of M31 as $V = 3.28$. Correcting for foreground extinction $A_V = 0.25$ (see Barmby et al. 2000) and our adopted value of $(m - M)_0 = 24.47$ gives $M_V = -21.43$, which is bracketed by the values given by van den Bergh (2000; $M_V = -21.2$) and Ashman & Zepf (1998; $M_V = -21.8$). For ease of comparison we use $M/L_V = 6.1$, as do Kissler-Patig et al. (1999). With $N_{gc} = 459 \pm 69$, this gives $S_N = 1.2 \pm 0.2$ and $T = 2.4 \pm 0.4$. Kissler-Patig et al. (1999) give S_N- and T-values for seven Sb–Sc spirals in addition to M31. The mean and dispersion of S_N and T for these galaxies are $\langle S_N \rangle = 0.8 \pm 0.2$ and $\langle T \rangle = 1.5 \pm 0.3$. For four Sa and Sab spirals, the (highly uncertain) mean values are $\langle S_N \rangle = 2.0 \pm 0.6$ and $\langle T \rangle = 4.0 \pm 1.1$. M31's values of S_N and T fall at the high end of the range of observed values for Sb and Sc spirals, and well within the range observed for Sa and Sab spirals. While it has about twice as many clusters per unit mass or luminosity than the Milky Way, M31 is within the range of variation seen in other spirals' GCSs. It is interesting to speculate on the difference between the Milky Way in M31 in terms of differences in the two galaxies' histories, since environmental differences obviously cannot be a major factor. Freeman (1999) suggested that M31 possibly suffered an early major merger; perhaps this was responsible for the creation of extra globular clusters in M31, as in the picture of Ashman & Zepf (1992). This would be consistent with the suggestion that some of the metal-rich globular clusters in M31 are younger than the rest of the population (Barmby & Huchra 2000; Barmby et al. 2001b), although there are not enough metal-rich clusters to account for the entire "cluster excess" in M31. Further explanation of the total number of clusters in M31 awaits both a larger spiral comparison sample and a more detailed theoretical picture of GCS formation.

6. SUMMARY

Using the *Hubble Space Telescope* Data Archive to search for M31 globular clusters in WFPC2 images, we present the discovery of many previously known clusters, a number of new cluster candidates, and some 20 objects that may be M31 open clusters. We use the discovery data, together with an estimate of our discovery efficiency, to estimate the completeness of existing cluster catalogs. As expected, the existing catalogs are least complete for faint clusters and clusters very near the center of M31. As we found in a preliminary version of this analysis in Barmby et al. (2001b), the completeness is very high to the magnitude limit we used for computing the globular cluster luminosity function. This validates our finding that the M31 GCLF varies both with radial distance from the center of M31 and with metallicity.

We use the completeness results to estimate the total number of globular clusters in M31 and derive values in the range 450–500, consistent with or somewhat higher than previous estimates. The specific frequency of globular clusters in M31 is $S_N = 1.2 \pm 0.2$, and the mass specific frequency $T = 2.4 \pm 0.4$. M31 has more clusters per unit mass or luminosity than the Milky Way but is within the range of specific frequencies seen in the limited number of other spirals studied to date.

We thank R. Di Stefano, J. Grindlay, D. Sasselov, and S. Zepf for helpful discussions.

REFERENCES

Ashman, K. A., & Zepf, S. E. 1992, ApJ, 384, 50
———. 1998, Globular Cluster Systems (Cambridge: Cambridge Univ. Press)
Barmby, P., Holland, S., & Huchra, J. P. 2001a, AJ, submitted
Barmby, P., & Huchra, J. P. 2000, ApJ, 531, L29
Barmby, P., Huchra, J. P., & Brodie, J. P. 2001b, AJ, 121, 1482
Barmby, P., Huchra, J. P., Brodie, J. P., Forbes, D. A., Schroder, L. L., & Grillmair, C. J. 2000, AJ, 119, 727
Battistini, P., Bònoli, F., Braccesi, A., Federici, L., Fusi Pecci, F., Marano, B., & Börngen, F. 1987, A&AS, 67, 447
Battistini, P. L., Bònoli, F., Casavecchia, M., Ciotti, L., Federici, L., & Fusi Pecci, F. 1993, A&A, 272, 77
Bertin, E., & Arnouts, S. 1996, A&AS, 117, 393
Crampton, D., Cowley, A. P., Schade, D., & Chayer, P. 1985, ApJ, 288, 494 (erratum 322, 1074 [1987]))
Djorgovski, S., & Meylan, G. 1993, in ASP Conf. Ser. 50, Structure and Dynamics of Globular Clusters, ed. S. G. Djorgovski & G. Meylan (San Francisco: ASP), 325
Dolphin, A. E. 2000, PASP, 112, 1397
Federici, L., Bònoli, F., Fusi Pecci, F., Marano, B., Lipovetsky, V. A., Neizvestny, S. I., & Spassova, N. 1993, A&A, 274, 87
Federici, L., Marano, B., & Fusi Pecci, F. 1990, A&A, 236, 99
Freeman, K. 1999, in IAU Symp. 192, The Stellar Content of Local Group Galaxies, ed. P. Whitelock & R. Cannon (San Francisco: ASP), 383
Harris, W. E. 1996, AJ, 112, 1487
Hodge, P. W. 1979, AJ, 84, 744
———. 1981, Atlas of the Andromeda Galaxy (Seattle: Univ. Washington Press)
Holland, S. 1998, AJ, 115, 1916
Holtzman, J. A., Burrows, C. J., Casertano, S., Hester, J. J., Trauger, J. T., Watson, A. M., & Worthey, G. 1995, PASP, 107, 1065
Hubble, E. 1932, ApJ, 76, 44
Huchra, J., Stauffer, J., & Van Speybroeck, L. 1982, ApJ, 259, L57
Huchra, J. P., Brodie, J. P., & Kent, S. M. 1991, ApJ, 370, 495
Hurt, R. L., Jarrett, T. H., Kirkpatrick, J. D., Cutri, R. M., Schneider, S. E., Skrutskie, M., & van Driel, W. 2000, AJ, 120, 1876
Kent, S. M. 1987, AJ, 94, 306
Kissler-Patig, M., Ashman, K. M., Zepf, S. E., & Freeman, K. C. 1999, AJ, 118, 197
Lee, M. G., Kim, S. C., Geisler, D., Seguel, J., Sarajedini, A., & Harris, W. E. 2001, in IAU Symp. 207, Extragalactic Star Clusters, ed. E. K. Grebel, D. Geisler, & D. Minniti (San Francisco: ASP), in press
Minniti, D. 1995, AJ, 109, 1663
Mochejska, B. J., Kaluzny, J., Krockenberger, M., Sasselov, D. D., & Stanek, K. Z. 1998, Acta Astron., 48, 455
Racine, R. 1991, AJ, 101, 865
Racine, R., & Harris, W. E. 1992, AJ, 104, 1068
Ratnatunga, K. U., Bahcall, J. N., & Casertano, S. 1989, ApJ, 339, 106
Sargent, W. L. W., Kowal, C. T., Hartwick, F. D. A., & van den Bergh, S. 1977, AJ, 82, 947
Seyfert, C. K., & Nassau, J. J. 1945, ApJ, 102, 377
Stanek, K. Z., & Garnavich, P. M. 1998, ApJ, 503, L131
Strauss, M. A., Huchra, J. P., Davis, M., Yahil, A., Fisher, K. B., & Tonry, J. 1992, ApJS, 83, 29
Supper, R., Hasinger, G., Pietsch, W., Trümper, J., Jain, A., Magnier, E. A., Lewin, W. H. G., & van Paradijs, J. 1997, A&A, 317, 328
van den Bergh, S. 2000, The Galaxies of the Local Group (Cambridge: Cambridge Univ. Press)
Vetešník, M. 1962, Bull. Astron. Inst. Czechoslovakia, 13, 180
Zepf, S. E., & Ashman, K. A. 1993, MNRAS, 264, 611
Zhang, X., Zhen, Y., Chen, H., & Wang, S. 1993, A&AS, 99, 545